Validating MOPITT Cloud Detection Techniques with MAS Images

Daniel Ziskin, Juying Warner, Paul Bailey, John Gille
National Center for Atmospheric Research, P.O. Box 3000, Boulder, CO 80307

ABSTRACT

The Measurements Of Pollution In The Troposphere (MOPITT) experiment will measure the amount of methane and carbon monoxide in the Earth's atmosphere utilizing spectroscopy in the near Infrared (IR) (2.2, 2.3, and 4.7 μm). In this wavelength region, clouds confound the retrieval of methane and carbon monoxide by shielding both the surface and atmospheric emission below the clouds from MOPITT. A technique has been developed to detect cloudy pixels, and an algorithm has been developed to estimate clear sky radiance from cloud contaminated pixels. This process is validated using images from the MODIS Airborne Simulator (MAS). MAS images are comprised of 50m pixels in comparison to the larger 22km MOPITT pixels. We aggregate the higher resolution MAS data to simulate MOPITT pixels. The aggregation is analyzed for clear and cloudy conditions and a cloud fraction is calculated. The aggregate is then averaged to recreate the scene that MOPITT would have seen. The cloud detection algorithms are applied to the degraded MAS image. The results are compared to validate the techniques imbedded in the standard MOPITT processing stream.

Keywords: MOPITT MAS CLOUD IMAGE IR

1. INTRODUCTION

The Measurements Of Pollution In The Troposphere (MOPITT) experiment will attempt to measure the amount of methane and carbon monoxide in the Earth's atmosphere.[1] The MOPITT retrieval algorithm[2] is based on correlative spectroscopy in the near Infrared (IR) (2.2, 2.3, and 4.7 μm). This instrument is mounted on NASA's Terra spacecraft[3], which is currently scheduled to launch late in the summer of 1999. It will orbit the earth in a near-polar sun-synchronous configuration at approximately 700km. From that height, virtually all the atmospheric CO and CH_4 in a cloud-free column should be visible to MOPITT. However, at these wavelengths clouds are not transparent. Clouds prevent either emitted or reflected radiation from gases below the clouds from reaching MOPITT. If this complication were ignored MOPITT retrievals would only detect the gases from above the cloud tops. The column amounts of CH_4 and CO would be grossly under-estimated. Therefore, being able to detect clouds and infer the amount of gas beneath them presents a challenge to the processing of MOPITT data. MOPITT addresses this problem with a cloud detection and cloud-clearing algorithm.[4]

1.1 Objective

An experiment was performed to validate the cloud detection and clearing techniques used in MOPITT processing. The goal is to demonstrate that cloudy pixels are accurately identified and that the clear-sky radiance for partially cloudy pixels is reasonably calculated.

1.2 Conclusion

Cloud detection and clearing will be possible when cloud amounts exceed 15% over well-characterized surfaces.

2. METHOD

2.1 MODIS Airborne Simulator (MAS)

MAS is an imaging spectrometer flown on a NASA ER-2 aircraft.[5] It has 50 spectral bands ranging from the visible through the IR. Its pixels are 50m in spatial extent. An array of 440x440 MAS pixels were averaged to simulate a single 22km MOPITT pixel. MAS data was selected for this experiment from the Winter Cloud Experiment (WINCE) performed over the Wisconsin region in January and February 1997. Three MAS spectral bands were selected, two to match MOPITT bands and a third for visual cloud detection. These MAS bands are summarized in Table 1, taken from the WINCE campaign web site (http://ltpwww.gsfc.nasa.gov/MAS/wince_bands50.html).

Table 1. MAS bands used to simulate MOPITT bands. All units are μm.

	MAS Band	MAS Peak	MAS Width at Half-Max	MOPITT Center	MOPITT Width
Solar CO (Solco)	24	2.353	0.048	2.334	0.022
Thermal CO	35	4.542	0.152	4.617	0.111
IR (cloud detection)	45	11.009	0.472	N/A	N/A

The flight selected occurred on February 12, 1997. From this flight we selected track 6, which began at 18:24:28 and ended at 18:53:58 GMT. This track began over eastern Minnesota (clear sky), then continued above Lake Superior. Initially, the lake was ice covered with a small patch of clouds. As the flight proceeded east, the ice broke up into mostly open water, with some ice. Clouds appeared in appreciable amounts over the lake water. The flight was divided into 25 MOPITT pixels (440x440 MAS pixels), and analysis was performed on the cloudy pixels over water. An image of this section of the flight is presented in Figure 1. The pixels were numbered from 0 to 24, but only the last seven were analyzed.

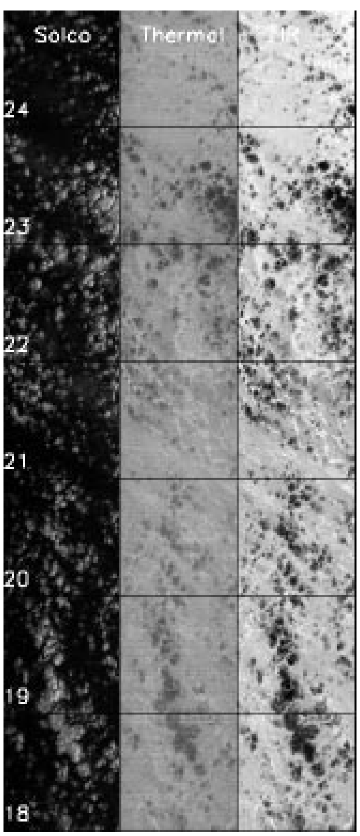

Figure 1. MAS data divided into MOPITT pixels over Lake Superior, February 12, 1997 18:45 GMT.

Once these pixels were identified, each was analyzed independently. The cloud amount was estimated using a combination of methods. These methods ranged from creating histograms of the data (number of pixels versus radiance in various bands) to subjective guessing. The success of various methods depended on the contrast between cloudy pixels and the surface, as well as factors such as the homogeneity of the underlying surface. The average radiance of all the pixels was calculated, which was meant to simulate what MOPITT would have seen. The clear sky radiance was also estimated. The clear sky radiance was estimated to be the peak radiance of the histogram of solar CO (i.e. the most likely reflected radiance), and the warmest pixel in the thermal channel. Histograms of a MOPITT pixel (pixel 20) are presented as Figures 2 and 3. The histogram of the solar CO channel illustrates that the surface radiance is sharply peaked and easily identifiable. This peak radiance is selected to represent the clear sky radiance in the solar CO channel. The broad-peaked histogram of the thermal channel indicates that the radiances from the surface and the clouds blend together. Thus, distinguishing clouds from the cold lake surface radiometrically is nearly impossible. The radiance from the warmest pixel is selected to represent the clear sky radiance in the thermal channel. These radiances are presented in Table 2.

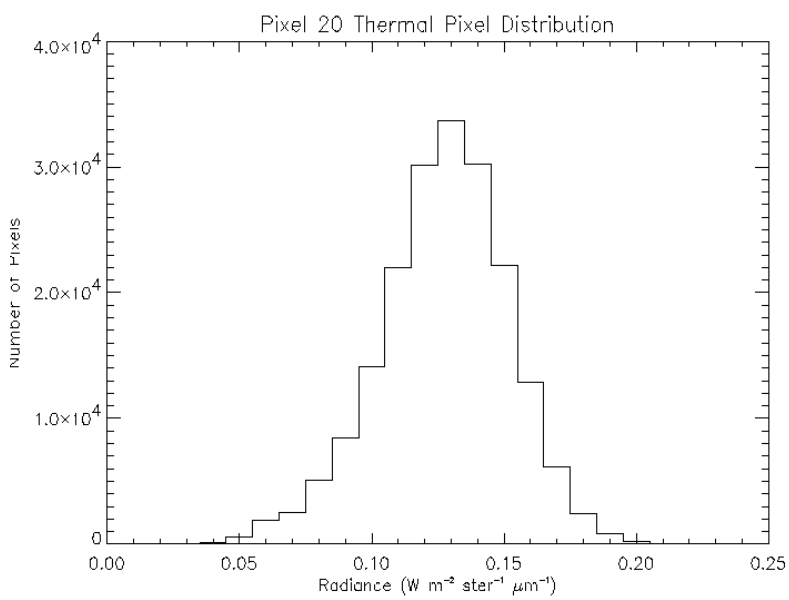

Figure 2. Histogram of thermal MAS pixels within MOPITT pixel 20. Note how clouds form a continuous distribution with the surface.

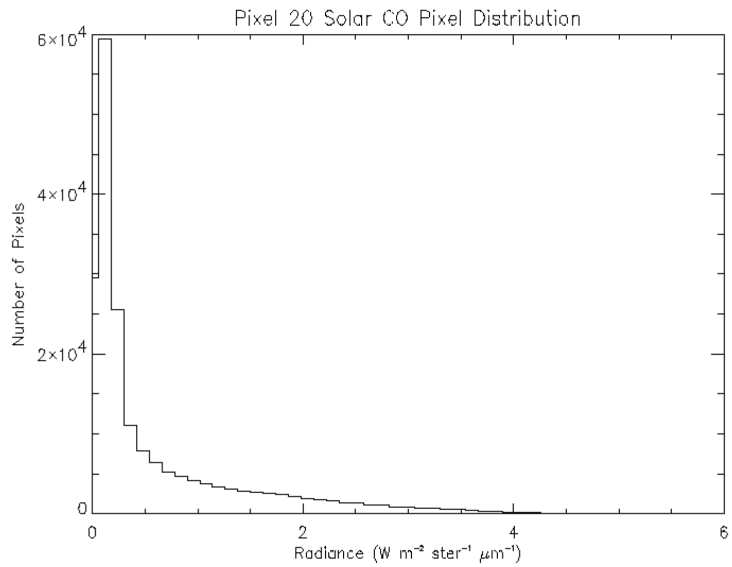

Figure 3. Histogram of solar CO MAS pixels within MOPITT pixel 20. Note how identifiable the surface radiance peak is.

Table 2. Average and Clear Sky Radiances from MAS data and model calculations. Cloudiness is also estimated.

MOPITT Pixel #	% Cloud	Average Thermal Radiance	Clear Sky Thermal Radiance	Model Thermal Clear Sky Radiance	Average Solar CO Radiance	Clear Sky Solar CO Radiance	Model Solar CO Clear Sky Radiance
18	27.2	0.17759	0.227	0.2374	0.75562	0.14	0.1485
19	32.3	0.17917	0.238	0.2374	0.7611	0.14	0.1485
20	36.4	0.18264	0.234	0.2374	0.66466	0.14	0.1485
21	18.1	0.18267	0.235	0.2374	0.69193	0.14	0.1485
22	40.3	0.17589	0.231	0.2374	1.03229	0.14	0.1485
23	35.8	0.17233	0.241	0.2374	1.02086	0.14	0.1485
24	17.3	0.18443	0.234	0.2374	0.49867	0.14	0.1485

Clear sky radiances were calculated with the MOPABS[6] model. This model uses an absorption look-up table approach. It accounts for the contribution from H_2O, CO_2, N_2O, CO, and CH_4. The profiles of CO_2, O_3, and N_2O are obtained from climatology. The profiles of CO and CH_4 were compiled from observations.

The model derived clear sky radiances were calculated with input of the surface temperature set to 267K and the surface emissivity set to 0.98 for both IR bands. The atmospheric profiles of water vapor and temperature were obtained from a radiosonde released as part of the WINCE[7] campaign. The sonde was released approximately 10 minutes after the images were taken from a location approximately 400km south (089 24.41'W, 43 04.17'N at 19:06:34 GMT). It is unlikely that the lake surface temperature was actually 6K below freezing, but this parameter was the temperature closest to the surface reported by the sonde. It is assumed that the surface temperature contains the uncertainty of the emissivity and the possibility of sub-pixel contamination by floating ice. The model results, which were parameterized to the MOPITT wave bands, were adjusted to match the spectral response of the MAS data (See Table 1). The relative error of approximately 6% in the solar CO channel and from 0.25% to 4.6% in the thermal channel suggests that the model is adequate for operational use. It also adds confidence that clear pixels would not be erroneously designated as cloudy. Since this experiment is an attempt to validate the MOPITT algorithm, rather than to actually determine the cloudiness of these pixels, all further calculations will treat the model calculations as the actual clear sky radiance. This will introduce model error into the analysis, with the advantage of being a more realistic scenario.

2.2 Cloud Detection

Cloud detection is based on the premise that clouds will reflect more radiation in the solar CO channel and emit less thermal radiation than the surface. By how much clouds alter the radiation at the top of the atmosphere is highly variable. Certainly any fixed threshold applied globally to detect clouds will contain errors. Selecting the most appropriate thresholds to minimize this source of error is particularly challenging. This experiment tests the currently selected thresholds. The ratio of observed radiance to clear sky radiance is calculated (and referred to as the "ratio test"). Also the difference between the clear sky radiance and the observed radiance is calculated ("difference test"). The ratio and difference tests are then compared to the pre-determined thresholds, which should indicate whether the pixel is cloudy or clear. The results of each of these tests are presented in Table 3. Since each pixel (except for one) exceeded the all thresholds set, these pixels would be classified as cloudy. Pixel 24 Solar CO Difference did not exceed the threshold set for cloudiness. However, the other three tests indicated that the pixel was cloudy. During operational MOPITT processing, if any one of these four tests indicates that a pixel is cloudy then it will be assumed to be cloudy. An attempt to radiometrically "clear" the effect of the clouds will be made before retrieval of CO or CH_4 is attempted on that pixel.

Table 3. The ratio and difference tests compared to threshold values of cloudiness

Pixel Number	Thermal Ratio	Solar CO Ratio	Thermal Difference	Solar CO Difference
18	0.748062	5.08835	0.05981	-0.60712
19	0.754718	5.125253	0.05823	-0.6126
20	0.769334	4.475825	0.05476	-0.51616
21	0.769461	4.659461	0.05473	-0.54343
22	0.740901	6.951448	0.06151	-0.88379
23	0.725906	6.874478	0.06507	-0.87236
24	0.776874	3.358047	0.05297	-0.35017
Threshold	< 0.93	> 3.0	> 0.05	< -0.5

3. ANALYSIS

What is the minimum cloudiness that this technique could detect? To answer this question a much larger sample size of pixels would be required. The following analysis simply demonstrates the method and presents a rough approximate answer. The radiance is cast as a linear function of cloud amount:

$$R_{obs} = R_{cld} \times f + R_{clr} \times (1 - f). \tag{1}$$

R_{obs} is the observed radiance, R_{cld} and R_{clr} are the cloudy and clear radiances respectively, and f is the cloud fraction. The ratio test can be represented as:

$$R_{obs}/R_{clr} = (R_{cld}/R_{clr} - 1) \times f + 1. \tag{2}$$

And the difference test can be represented as:

$$R_{clr} - R_{obs} = (R_{clr} - R_{cld}) \times f. \tag{3}$$

Both of these tests are linear functions of f, where the slope and intercept can be empirically calculated. The results are presented in Table 4 and Figure 4.

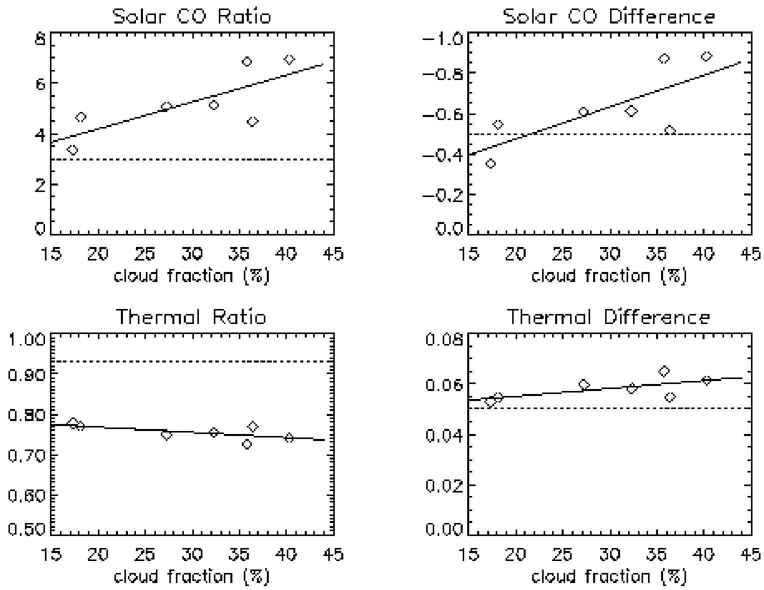

Figure 4. The ratio and difference tests for the thermal and solar CO bands as a function of cloud fraction. The solid line is the least-squares linear fit. The dashed line is the threshold. Note that the thermal ratio and solar CO difference tests would require a negative cloud fraction to register as clear pixels.

Table 4. The derived slopes and intercepts of the various tests as a function of cloud fraction. The slope is in terms of cloud fraction (0-1) rather than percent (0-100). The threshold value is an estimate of the minimum cloudiness detectable by this method. Negative threshold values imply that any pixel (regardless of cloudiness) would have been classified as cloudy.

	Thermal Ratio	Solar CO Ratio	Thermal Difference	Solar CO Difference
Slope	-0.13	10.7	0.031	-1.59
Intercept	0.79	2.04	0.049	-0.15
Threshold (%)	-103.2	8.9	3.6	21.7

4. Conclusion

4.1 Error Analysis

This particular experiment stressed the cloud detection tests because the cold surface temperature reduced the contrast between clouds and the surface in the thermal channels. This could account for the poor performance of the thermal ratio test. Surprisingly, the thermal difference test proved to be one of the most sensitive. Perhaps the reason the thermal difference test was more successful than the thermal ratio test was the way model error (primarily due to uncertainty in the emissivity and surface temperature) is propagated through the test. The thermal difference test, as expressed in equation (3), indicates that model errors should be linear with cloud fraction. So at small cloud amounts, the error propagated to the difference should also be small. Whereas, errors in the model are not linear in the ratio test as written in equation (2).

The solar CO tests were expected to perform better than the thermal tests, since the contrast between clear and cloudy MAS pixels was higher in this wave band. The solar CO ratio test did yield a more realistic threshold value than its thermal counterpart. Errors in the surface temperature and emissivity, propagated through model-calculated clear sky radiance, probably had a larger effect on the solar CO tests. As seen in Table 2, the model radiance is 6% higher than the observed clear sky radiance.

4.2 Prognosis for MOPITT

These techniques appear quite adequate for detecting clouds under operational circumstances. Clearly, there will be some challenging scenes that any automated algorithm will fail. These tests also provided insight into the conservative nature of the selected thresholds. Under these conditions, it is more likely that clear pixels would be designated as cloudy than vice-versa. A bias in this direction will produce higher quality data in the initial stages of MOPITT production.

ACKNOWLEDGEMENTS

The National Aeronautics and Space Administration Earth Observing System (EOS) Program funded this work under contract NAS5-30888. MAS data was provided by the NASA Goddard DAAC. The radiosonde profile was obtained from the WINCE web site. Thanks are offered to Liam Gumley for providing excellent access software to MAS data. Dave Grant and Dan Packman of the MOPITT team also provided assistance.

REFERENCES

1. J. R. Drummond, “Measurements Of Pollution In The Troposphere (MOPITT)”, *The Use of EOS for Studies of Atmospheric Physics*, J. C. Gille and G. Visconti, Eds., North-Holland, New York, pp. 77-101, 1992.
2. L. Pan, J. C. Gille, D. P. Edwards, P. Bailey, “Retrieval of Tropospheric Carbon Monoxide for the MOPITT Experiment”, JGR, 103:32,777-32,290, 1998.
3. G. Asrar, J. Dozier, *Science Strategy for the Earth Observing System*, AIP Press, 1994.
4. J. Warner, J. C. Gille, D. Edwards, P. Bailey, “Cloud Detection and Clearing for the MOPITT Instrument”, SPIE International Symposium on Optical Science, Engineering, and Instrumentation, Denver, 1999.
5. L. E. Gumley, P. A. Hubanks, E. J. Masuoka, “MODIS Airborne Simulator Level 1B Data User’s Guide”, NASA Technical Memorandum 104594, Vol. 3, 1994.
6. D. P. Edwards, C. Halvorson, J. C. Gille, “Radiative Transfer Modeling for the EOS Terra Satellite Measurements Of Pollution In The Troposphere (MOPITT) Instrument”, J. Geophys. Res., in press, 1999.
7. S. A. Ackerman, C. C. Moeller, W. P. Menzel, J. D. Spinhirne, D. Hall, J. R. Wang, H. E. Revercomb, R. O. Knuteson, E. W. Eloranta, A. W. Nolin, and M. D. King, "WINCE, a winter cloud experiment", 10th Conference on Atmospheric Radiation, Madison, WI, AMS, June 26 - July 2, 1999.